IOP Conference Series: Earth and Environmental Science

PAPER • **OPEN ACCESS**

Effects of stern-foil submerged elevation on the lift and drag of a hydrofoil craft

To cite this article: K Suastika and Apriansyah 2018 *IOP Conf. Ser.: Earth Environ. Sci.* **135** 012003

View the article online for updates and enhancements.

You may also like

- Optimal design of aeroacoustic airfoils with owl-inspired trailing-edge serrations
Mingzhi Zhao, Huijing Cao, Mingming Zhang et al.
- Development of a morphing flap using shape memory alloy actuators: the aerodynamic characteristics of a morphing flap
Seung-Hee Ko, Jae-Sung Bae and Jin-Ho Rho
- Thermoelectric effect and a thermoelectric generator based on carbon nanostructures: achievements and prospects
E D Eidelman

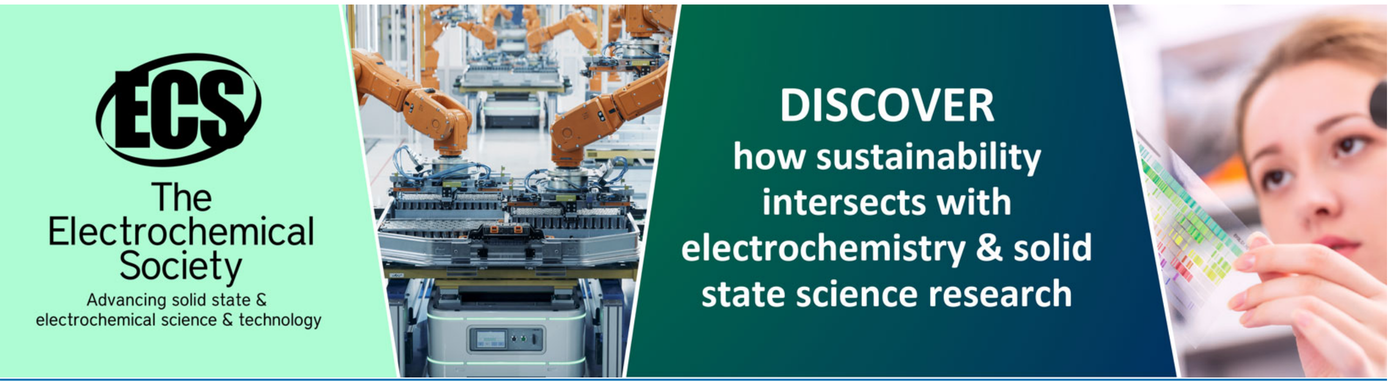

This content was downloaded from IP address 3.23.101.91 on 17/05/2024 at 15:43

IOP Conf. Series: Earth and Environmental Science **135** (2018) 012003 doi:10.1088/1755-1315/135/1/012003

Effects of stern-foil submerged elevation on the lift and drag of a hydrofoil craft

K Suastika[1] and Apriansyah[1]

[1]Department of Naval Architecture and Shipbuilding Engineering, Faculty of Marine Technology, Institut Teknologi Sepuluh Nopember (ITS), Kampus ITS Sukolilo, Surabaya 60111, Indonesia

Email: k_suastika@na.its.ac.id

Abstract. Effects of the stern-foil submerged elevation on the lift and drag of a hydrofoil craft are studied by using computational fluid dynamics (CFD) and by considering three alternative stern-foil submerged elevations. The submerged elevation of the front foil is kept constant in all the alternatives. From among the alternatives, the deepest stern-foil placement results in the highest stern-foil lift with the highest foil's lift-to-drag ratio. However, considering the lift-to-drag ratio of the whole foil-strut-hull system, the shallowest stern-foil placement results in the highest lift-to-drag ratio. The struts and the foil's submerged elevation significantly affects the drag of the whole foil-strut-hull system.

1. Introduction

The use of a hydrofoil on a boat is particularly aimed at reducing the viscous resistance of the boat while moving in the water. At relatively high speed the hydrofoil can produce a sufficient lifting force so that the hull can be lifted out of the water, thus reducing the ship's wetted surface area (WSA) and the ship's resistance. Besnard et al. [1] conducted research to gain the maximum lift-to-drag ratio of hydrofoils to be applied to fast boats. They used a panel method to calculate the 3-D flow field, taking into account free-surface effects. The numerical tool is integrated into a multi-criteria optimization method applied for the design of a single and biplane foils. Considering vessel's maneuvering, Latorre and Teerasin [2] calculated the take-off speed of hydrofoil vessels with different foil size and angle of attack. Calculation results show that different regions of the foil are exposed to a large impact at the take-off. Putnam et al. [3] performed tests to select the most optimum type of foil that will be used for hydrofoil boats. As parameter for best performance is the maximum lift-to-drag ratio. Different foil types were studied and they recommended Eppler-396 foil for the stern foil and Eppler-420 for the front foil of the hydrofoil craft.

Saputro and Suastika [4] conducted model experiments of a hydrofoil craft in a towing tank and varied the positions of the front- and stern foils in the longitudinal direction. They reported an optimum placement of the foils with the smallest resistance but the lifting of the bow was not followed by the stern. It is suggested that this is due to the alignment of the two foils relative to the water line, which was at the same elevation. This results in that the flow of water that passes the stern foil has been affected by the turbulence generated by the front foil such that the lifting capacity of the stern foil is markedly reduced.

The purpose of present study is to investigate effects of the stern-foil submerged elevation of a hydrofoil craft on the lift and drag. The same vessel is considered as in [4]. The vessel's principal dimensions are summarized in table 1. The submerged elevation of the front foil is kept constant but

Content from this work may be used under the terms of the Creative Commons Attribution 3.0 licence. Any further distribution of this work must maintain attribution to the author(s) and the title of the work, journal citation and DOI.
Published under licence by IOP Publishing Ltd

that for the stern foil is varied in the vertical direction, for which three alternatives are investigated (see figure 1 and table 2). Following Saputro and Suastika [4], both the front and the stern foils are NACA 64(1)212 foils while the struts are NACA 63012 symmetrical foils.

To obtain the most optimum foil size, CFD-simulations were done of foil alone with varying foil's aspect ratio (AR) and angle of attack. The aspect ratio is defined as [5]:

$$AR = \frac{(b)^2}{S} = \frac{b}{c} \tag{1}$$

$$AR = \frac{b}{c}\left[1 + \left(\frac{a}{b}\right)^3\right]\frac{h}{b} \tag{2}$$

where a is the breadth of the craft, b is the foil span, c is the chord length, h is the submerged elevation of the foil below the water line and S is the foil area. Equation (1) is used for calculating the foil aspect ratio (to lift the vessel) while equation (2) for the strut aspect ratio. The range of recommended aspect ratio for a hydrofoil is between 4 and 10 [6]. Then, simulations with foils attached to the hull are done to study effects of the stern-foil submerged elevation on the lift and drag of the hydrofoil craft.

Table 1. Vessel's principal dimensions.

Length overall (L_{OA})	15.85	m
Length of water line (L_{WL})	14.48	m
Beam (B)	4.00	m
Draft (T)	0.70	m
Height (H)	1.80	m
Displacement (∇)	18.75	ton

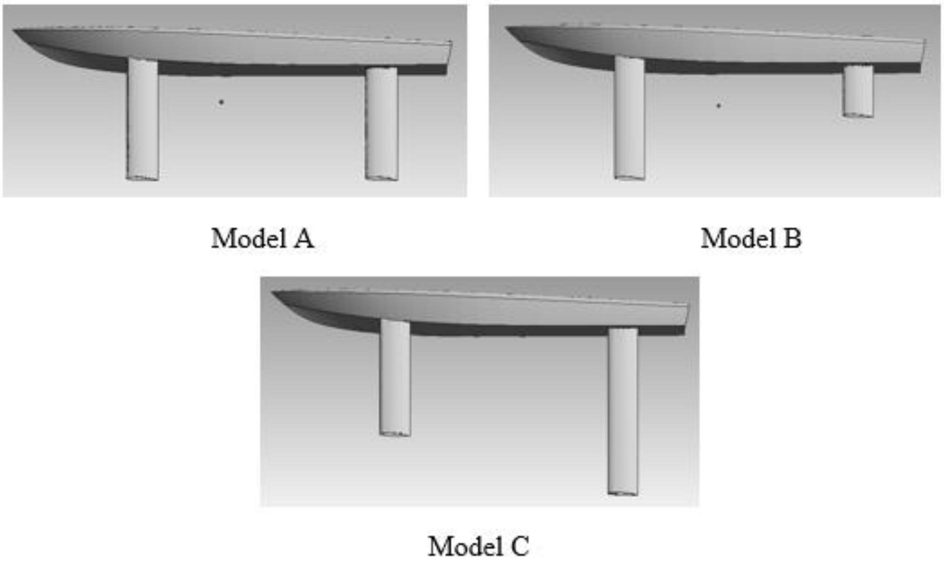

Figure 1. Three alternatives for the stern-foil submerged elevation with constant front-foil elevation.

Table 2. Submerged elevation of the front and stern foils below the water surface.

	Front foil	**Stern foil**
Model A	6.37 T = 4.46 m	6.37 T = 4.46 m
Model B	6.37 T = 4.46 m	3.19 T = 2.23 m
Model C	6.37 T = 4.46 m	9.56 T = 6.69 m

2. Foil-size optimization

Based on the location of the center of gravity (LCG) and the positions of the front- and stern foils in the longitudinal direction, the required lift for both the front and stern foils can be calculated. Calculation results show that the required lift for the front foil is 85.66 kN while that for the stern foil is 98.09 kN. To obtain the optimum foil size, CFD-simulations of foil alone were done. Two foil spans are considered, namely 4.0 m (the same as the vessel's beam) and 5.0 m. The Froude number used in the simulations is $Fr = 0.8$, corresponding to a vessel's speed of 9.53 m/s (18.53 knots).

2.1. Meshing, boundary conditions and the turbulence model

Figure 2 shows a mesh of the NACA 64(1)212 foil and figure 3 the position of the hydrofoil model in the computational domain. Grid-independence tests [7] were done to obtain the most optimum grid size. Test results show that the optimum number of elements for the simulations is 1,074,984. The root mean square (rms) error criterion with a residual target value of 10^{-6} is used as the criterion for the convergence of the numerical solutions.

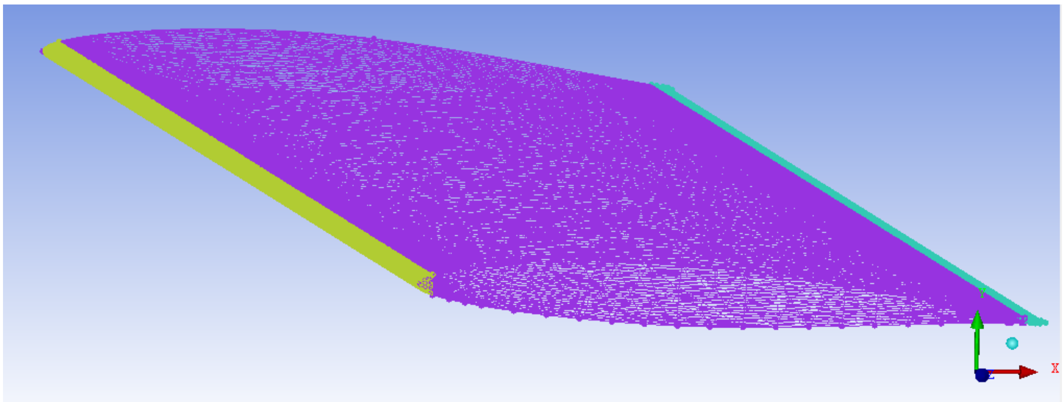

Figure 2. Mesh of NACA 64(1)212 foil used for the hydrofoil craft.

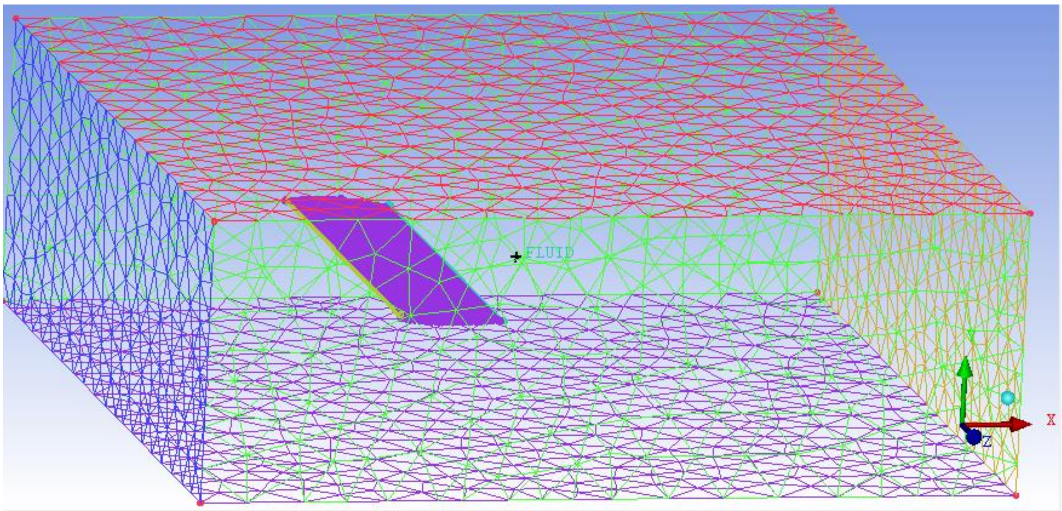

Figure 3. Position of the foil in the computational domain.

The boundary conditions of the computational domain are as follows [8]. The condition at the inlet boundary, located 2-*c* upstream from the leading edge (*c* is the chord's length), is defined as a uniform flow with velocity equalling the vessel's speed (in the simulations, the vessel is at rest while the fluid is flowing). The boundary condition at the outlet, located 5-*c* downstream from the trailing edge, is defined such that the pressure is equal to the undisturb static pressure. The boundary condition on the surface (wall) of the foil is defined as no-slip boundary (smooth wall). The boundary condition at the side walls is defined as a symmetric pressure condition, that is, the pressure on the inside wall is equal to that on the outside wall. Finally, the boundary conditions at the top (2-*c* above the upper surface of the model) and the bottom (2-*c* below the lower surface of the model) surfaces are defined as free-slip boundaries. Free surface effects (generation of waves) are not modeled in this case (foil alone).

The turbulence model used in the simulations of foil alone is the k-ε model [9, 10].

2.2. Results of foil-alone simulations

Figure 4 shows plots of lift-to-drag ratio as function of angle of attack (α) for foils with 4-m span and different chord lengths, while figure 5 shows lift-to-drag ratio plots for foils with 5-m span. In all cases, the aspect ratio is kept within the recommended range, namely, between 4 and 10 [6] (see tables 3 and 4). Figures 4 and 5 show that the lift-to-drag ratio increases monotonically with increasing angle of attack and then decreases. The maximum value of lift-to-drag ratio (stall) takes place at the angle of attack of approximately 3.5 degrees. The most optimum foil with 4-m span is that with chord's length of 0.43 m (AR = 9.39) while the most optimum foil with 5-m span is that with chord's length of 1.14 m (AR = 4.40).

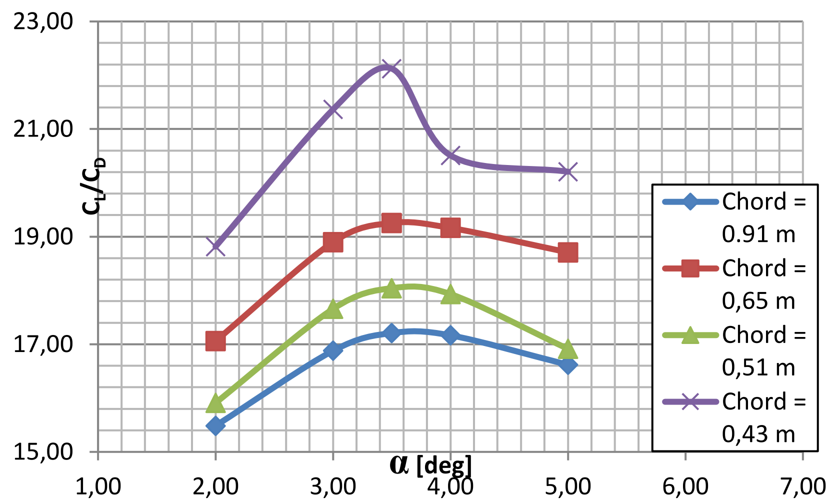

Figure 4. Lift-to-drag ratio as function of angle of attack for foils with 4-m span and different chord's lengths.

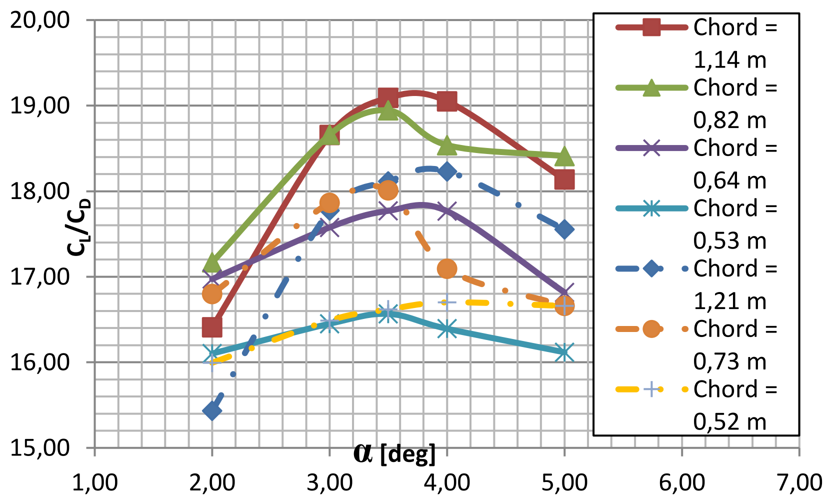

Figure 5. Lift-to-drag ratio as function of angle of attack for foils with 5-m span and different chord's lengths.

Table 3. Foil's lift at Fr = 0.8 and α = 3.5° for 4-m foil's span.

Chord [m]	AR	Lift [kN]
0.91	4.40	60.22
0.65	6.13	49.52
0.51	7.83	40.52
0.43	9.39	35.77

Table 4. Foil's lift at Fr = 0.8 and α = 3.5° for 5-m foil's span.

Chord [m]	AR	Lift [kN]
1.14	4.40	83.22
1.21	4.14	82.68
0.82	6.13	81.61
0.73	6.87	79.28
0.64	7.83	79.28
0.53	9.39	84.03
0.52	9.57	76.27

Tables 3 and 4 summarize results of lift force calculations with Fr = 0.8 and α = 3.5° for 4-m foil's span and for 5-m foil's span, respectively. Tables 3 and 4 show that the lifts generated by the foils with 4-m span are smaller than those generated by the 5-m span foils, as expected. In both cases (4-m and 5-m spans), the generated lifts are smaller than the required lifts (85.66 kN for the front foil and 98.09 kN for the stern foil).

To provide a sufficient lift for foilborne, the foil's span can be increased but AR must be kept within the recommended range. Another option is to keep the foil's span remaining 5.0 m but foilborne is expected to take place at a larger Froude number. The latter option is chosen in the present study. Thus, the foil to be used is NACA 64(1)212 foil with 5-m span and chord of 1.14 m (AR = 4.40).

3. Foils attached to hull

To study effects of the stern-foil submerged elevation on the lift and drag of the hydrofoil craft, simulations were done with foils attached to the hull (by using struts). In the simulations, the foil's angle of attack (both the front and stern foils) was set 3.5° (see section 2). Furthermore, different Froude numbers are considered, namely, Fr = 0.8, 0.9, 1.0, 1.1 and 1.2.

3.1. Meshing, boundary conditions and the turbulence model

Figure 6 shows a mesh of the hydrofoil craft for model B while figure 7 shows the position of the hydrofoil-craft model in the computational domain. Grid-independence tests [7] were done to obtain the most optimum grid size. Test results show that the optimum number of elements for the simulations is 1,791,588. The root mean square (rms) error criterion with a residual target value of 10^{-4} is used as the criterion for the convergence of the numerical solutions.

The boundary conditions are as follows [8]. At the inlet, located at 2-L upstream from the vessel (L is the vessel's length), the condition is defined as a uniform flow with velocity equalling the vessel's speed (in the simulations, the vessel is at rest while the fluid is flowing). The boundary at the outlet (5-L downstream from the vessel) is defined such that the pressure is equal the undisturbed static pressure. The boundary condition on the wall of the vessel is defined as no-slip boundary (smooth wall). The boundary conditions at the bottom wall (2-L below the vessel) and the top wall (2-L above the vessel) are defined as free-slip condition. Free-surface effects (interface between water and air; generation of waves) are modeled in this case (foils attached to hull). The viscous-flow field is solved using Reynold's averaged Navier-Stokes (RANS) solver for incompressible flow.

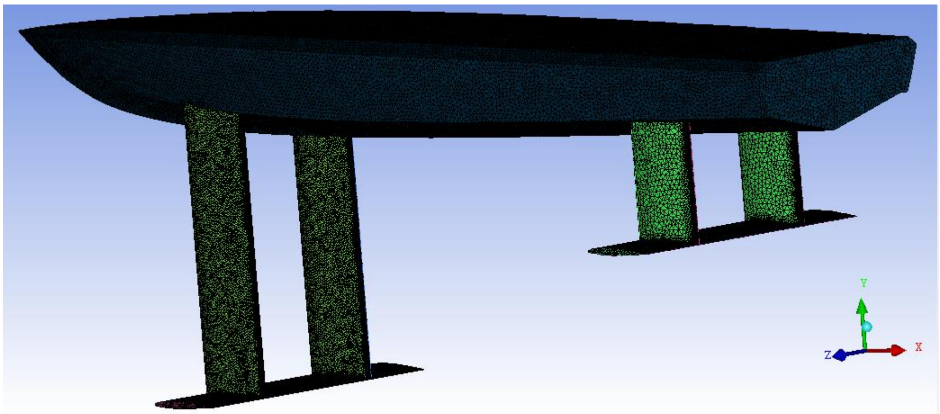

Figure 6. Mesh of the hydrofoil craft for model B.

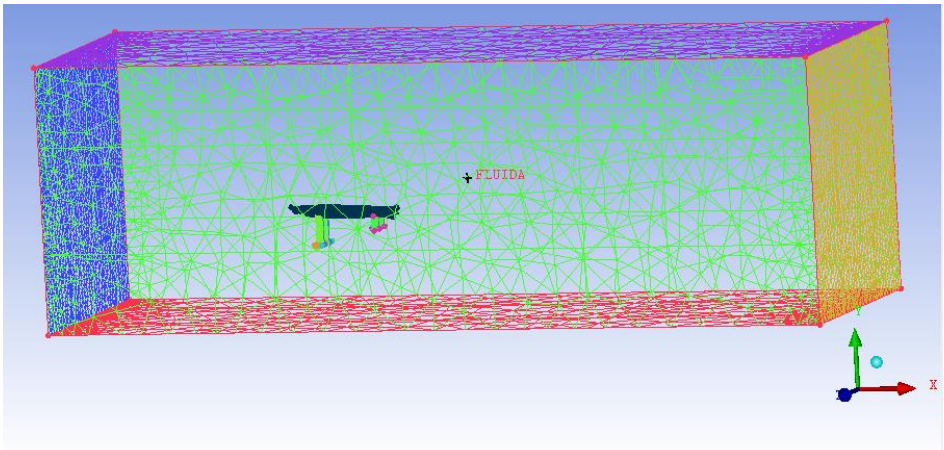

Figure 7. Position of the hydrofoil-craft model in the computational domain.

The turbulence model used is the SST k-ω model [9]. This turbulence model, which is a hybrid model utilizing a k-ω model for the turbulent boundary layer flow and a k-ε model for the flow outside the boundary layer, has been succesfully applied in many applications [10, 11].

3.2. Results of foils attached to hull

Tables 5, 6 and 7 summarize the lift forces for the front and stern foils for *Fr* = 0.8, 0.9 and 1.0, respectively. Recall that the required lift for the front foil is 85.66 kN while that for the stern foil is 98.09 kN. At *Fr* = 0.8 and 0.9, the lift forces of the front and/or the stern foils are smaller than the respectively required lifts. At *Fr* = 1.0, models B and C provide sufficient lift for the vessel to foilborne. The highest lift-to-drag ratio of the stern foil in the range of *Fr* between 0.8 and 1.1 is given by model C (see figure 8). However, looking at the lift-to-drag ratio of the whole foil-strut-hull system, model B gives the highest lift-to-drag ratio (see figure 9). If the lift-to-drag ratio of the whole foil-strut-hull is considered as parameter for best performance, model B is the best alternative, for which the vessel is expected to foilborne at *Fr* approximately 1.0 (see table 7).

Table 5. Lift forces of the front and stern foils (*Fr* = 0.8).

Model	Front Foil [kN]	Stern Foil [kN]	Difference [%]
A	84.87	66.84	26.98
B	80.11	72.59	10.36
C	81.21	76.16	6.64

Table 6. Lift forces of the front and stern foils (*Fr* = 0.9).

Model	Front Foil [kN]	Stern Foil [kN]	Difference [%]
A	106.21	79.42	33.73
B	100.61	85.89	17.15
C	103.58	92.66	11.78

Table 7. Lift forces of the front and stern foils (*Fr* = 1.0).

Model	Front Foil [kN]	Stern Foil [kN]	Difference [%]
A	129.83	95.05	36.58
B	123.06	104.61	17.63
C	127.38	110.26	15.53

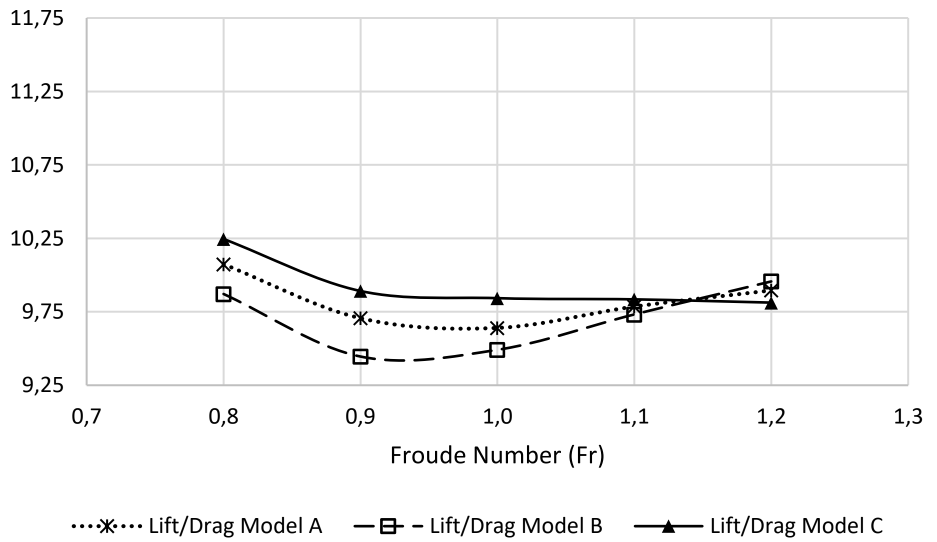

Figure 8. Lift-to-drag ratio of the stern foil for model A, B and C.

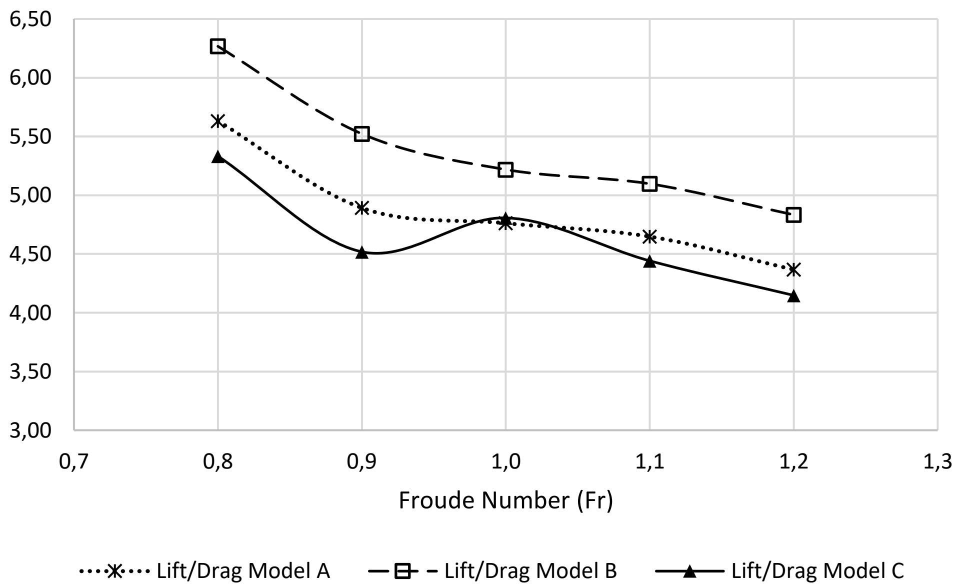

Figure 9. Lift-to-drag ratio of the hydrofoil craft for model A, B and C.

4. Conclusions

Based on the required lift, the recommended foil's aspect ratio and the highest lift-to-drag ratio, the foil chosen for the hydrofoil craft is NACA 64(1)212 with 5-m span and chord of 1.14 m (AR = 4.40). Simulation results of foils attached to the hull show that the stern-foil submerged elevation significantly influences the lift generated by the stern foil. Setting the stern foil deeper than the front foil (model C) or shallower than the front foil (model B) result in a larger lift for the stern foil. The above result support the hypothesis that the front foil significantly affects the flow upstream from the stern foil that can result in a reduction of the lifting capacity of the stern foil. Among the three alternatives considered, model C results in the highest lift and the highest lift-to-drag ratio for the stern foil. However, considering the whole foil-strut-hull system, model B with the shortest strut gives the highest lift-to-drag ratio of the hydrofoil craft. Clearly, the struts and the foil's submerged elevation significantly affects the total drag of the system. If the lift-to-drag ratio of the whole system is used as parameter for best performance, then model B is the most optimum alternative.

Acknowledgment

This research project was financially supported by the Indonesian Ministry of Research and Higher Education (RISTEKDIKTI), under the grant: Penelitian Kerjasama Industri 2017.

References

[1] Besnard E, Schmitz A, Kaups K, Tzong G, Hefazi H, Kural O, Chen H and Cebeci, T 1998 Hydrofoil design and optimization for fast ships, *Proc. 1998 ASME Int. Congress Exhibition* (Anaheim, USA)

[2] Latorre R and Teerasin S 1992 Calculation of hydrofoil craft take-off speed including influence of foil size, foil angle and propeller shaft angle *Ocean Engng* **9**(2) 183

[3] Putnam N, Dickert G and Wagner C 2014 On the Design, Construction, and Testing of a Fully-Submerged Canard Hydrofoil System for a Low-speed Solar Boat, Elmer W. Engstrom Department of Engineering and Computer Science, Cedarville University, Cedarville

[4] Saputro S A and Suastika K 2012 Kajian eksperimental pengaruh posisi perletakan hydrofoil pendukung terhadap hambatan kapal *J Teknik ITS* **1**(1) G-51

[5] Du Cane P 1974 *High Speed Small Craft* (Portland: David & Charles)

[6] van Walree F 1999 *Computational Methods for Hydrofoil Craft in Steady and Unsteady Flow*, Ph.D.-thesis, Delft University of Technology, The Netherlands

[7] Anderson, J D 1995 *Computational Fluid Dynamics: The Basics with Applications* (New York: McGraw-Hill, Inc.)

[8] Versteeg H K and Malalasekera W 2007 *An Intoduction to Computational Fluid Dynamics: The Finite Volume Method* (United Kingdom: Longman Scientific)

[9] Menter, F R 1994 Two-equation eddy-viscosity turbulence models for engineering applications *AIAA J* **32**(8) 1598

[10] Mordhorst C J 2001 Investigation of Open Source CFD Software on Shipyards, M.Sc.-thesis, Chalmers University of Technology, Sweden

[11] Swennberg S U 2000 A test of turbulence models for steady flows around ship, *Proc. Gothenburg Workshop on Numerical Ship Hydrodynamics* (Gothenburg)